The Electrical Conductivities of the DSS-13 Beam-Waveguide Antenna Shroud Material and Other Antenna Reflector Surface Materials

T. Y. Otoshi, M. M. Franco, and H. F. Reilly, Jr.
Ground Antennas and Facilities Engineering Section

A significant amount of noise temperature can potentially be generated by currently unknown dissipative losses in the beam-waveguide (BWG) shroud. The amount of noise-temperature contribution from this source is currently being investigated. In conjunction with this study, electrical conductivity measurements were made on samples of the DSS-13 BWG shroud material at 8.420 GHz. The effective conductivities of unpainted and painted samples of the BWG shroud have been measured to be 0.01 × 10^7 and 0.0036 × 10^7 mhos/m, respectively. This value may be compared with 5.66 × 10^7 mhos/m for high-conductivity copper.

I. Introduction

A description of the DSS-13 beam-waveguide (BWG) antenna as well as experimental noise temperature data have been presented in a Phase I Final Report.[1] Although antenna efficiencies agreed well with predictions, measured operating noise temperatures for the BWG portion of the system at 8.45 GHz were found to be about 6 K higher than had been expected.

The causes of the noise temperatures generated within a BWG antenna are currently under investigation. A possible cause of noise increase being studied is the dissipative loss in the walls of the BWG steel shroud. The shroud, 2.44 m in diameter and about 24.4 m long, begins at the Cassegrain vertex and, after four 90-deg turns, ends at the antenna azimuth plane. Then, for about 1.5 m, between the azimuth plane down to the ceiling of the pedestal room, the shroud wall is made of concrete instead of steel. The remainder of the microwave path to the final focal point F3 is unshrouded.

Little information is available in the technical literature concerning the electrical conductivity values of various types of steel at microwave frequencies. It is the purpose of this article to summarize all known published data on the conductivity values of many types of steel materials. Most of the values to be presented were obtained from

[1] M. Britcliffe, Editor, *DSS-13 Beam Waveguide Antenna Project: Phase 1 Final Report*, JPL D-8451 (internal document), Jet Propulsion Laboratory, Pasadena, California, May 15, 1991.

JPL experimental data previously reported in the form of insertion loss and surface resistivity values. For this article, these experimental data were converted to electrical conductivity values. Data will also be presented on recently measured conductivity values of four test samples of the DSS-13 BWG steel shroud material.

II. Previous Test Data

Table 1 is a summary of all known previous experimental data on the electrical conductivity values of various types of steel at various microwave frequencies. In this table one can see that the experimental values at microwave frequencies range from a minimum of 0.0036×10^7 mhos/m to a maximum of 0.148×10^7 mhos/m, as compared with the dc value of 0.5×10^7 mhos/m. For purposes of comparison, the conductivity value of oxygen-free high-conductivity copper at microwave frequencies is 5.66×10^7 mhos/m, as compared with 5.8×10^7 mhos/m at dc. The term "effective conductivity" in Table 1 is the actual conductivity value divided by the relative permeability value. The relationships of permeability to surface resistivity and skin depth will be shown below.

From basic electromagnetic theory [8], it can be shown that the surface resistivity of a conductor in ohms/square is given as

$$R_s = 20\pi\sqrt{\frac{f_{\mathrm{GHz}}\mu_r}{\sigma}} \tag{1}$$

where f_{GHz} is the frequency in GHz, μ_r is the relative permeability, and σ is the electrical conductivity in mhos/m.

By defining effective conductivity as

$$\sigma_{\mathrm{eff}} = \frac{\sigma}{\mu_r} \tag{2}$$

Eq. (1) then becomes

$$R_s = 20\pi\sqrt{\frac{f_{\mathrm{GHz}}}{\sigma_{\mathrm{eff}}}} \tag{3}$$

If R_s is known at the measurement frequency but the effective conductivity is the parameter to be determined, one can use the following expression that was derived from algebraic manipulation of Eq. (3):

$$\sigma_{\mathrm{eff}} = \left(\frac{20\pi}{R_s}\right)^2 f_{\mathrm{GHz}} \tag{4}$$

where σ_{eff} is expressed in units of mhos/m.

The expression for skin depth in microinches can be derived as

$$\delta_{\mu i} = \frac{9972.58R_s}{f_{\mathrm{GHz}}\mu_r} \tag{5}$$

For the steel sample in Table 1, an effective conductivity of 0.0036×10^7 mhos/m was measured at 3.015 GHz. Since conductivity is approximately constant at microwave frequencies (except for surface-roughness and skin-depth effects), a calculation can be made by using this conductivity value for other microwave frequencies. Then for $f_{\mathrm{GHz}} = 8.45$, from Eq. (3), $R_s = 0.9626$ ohms/square. If it is assumed that $\mu_r = 150$, then from Eq. (5), the skin depth is 7.57 μin. However, if $\mu_r = 1000$, the skin depth becomes 1.14 μin. For comparison purposes, it is of interest to make a similar calculation of a nonmagnetic material, such as aluminum, for $\mu_r = 1.0$ and a typical conductivity σ of 2.2×10^7 mhos/m. Then, at 8.45 GHz, $R_s = 0.0389$ ohms/square, and the skin depth is about 46 μin.

It is known that at microwave frequencies, conductivity losses will increase with the increase of the ratio of surface roughness to skin depth [9]. Therefore, based on the previous discussion, one would expect the losses of a magnetic steel material with high permeability and a poor surface finish to have relatively high losses at microwave frequencies. As Vane points out, "Metals which have relatively high permeability are particularly lossy because the skin depth decreases with increasing permeability, thereby heightening the importance of surface irregularities." [1]

For interest, Table 2 is a tabulation of chemical composition and relative permeability values of stainless steel types 303, 304, 321, and 347. These are the types of stainless steel for which measured effective conductivity values are given in Table 1. It can be seen from Table 2 that the relative permeability values of these types of stainless steel are low (close to unity) and vary from 1.0–1.70. The relative permeability values of most types of stainless steel are functions of percent cold work reduction, but are generally less than 1.5. An exception is type 321 stainless steel whose relative permeabilty value has been measured to be as high as 9.4 for 71-percent cold work reduction and a magnetizing force of 200 Oe. Based upon these data, it can be stated that for most types of stainless steel materials,

the permeability will have little effect on the dissipative losses.

In contrast to the low magnetic properties of stainless steels, the relative permeability values of some types of carbon steel can be as high as 3000.[2] The relative permeability values of most structural or high-carbon-content steel are quite variable. If permeability of a particular type of steel must be known accurately, then the permeability values of samples of the particular material to be used need to be measured individually.

Since it was of interest to know the relative permeability of the DSS-13 shroud material, a sample of the material was given to the JPL Magnetics Test Laboratory for measurements of permeability. However, after several attempts using different methods, it was concluded that JPL does not currently have the equipment needed to measure permeability values of high-permeability steels.

III. Measurement Technique

A. Description of Technique

The TE_{011} mode resonant-cavity technique employed to obtain the test results for this article was basically the same as that described previously [6,11], except that an HP 8510C Automatic Network Analyzer (ANA) was employed. Insertion losses at precisely known frequencies can be measured more accurately and more rapidly with the HP 8510C than with the nonautomated methods employed in the past. With the ANA, upon command, the computer finds the frequency of minimum insertion loss and the frequencies of the 3-dB points to 0.1-KHz resolution, as compared with 1-KHz resolution previously obtained with other setups. Insertion loss can be measured to 0.02-dB resolution. Visual displays of loss versus frequency are available on-screen, and an option is available for real-time hard copies of the frequency–response plots of the type shown in Fig. 1. The data can be stored for post-processing, later verifications and plotting, if desired. The application of the ANA for cavity measurements is considered to be a technical innovation that advances the state-of-the-art of reflector surface material evaluations.

B. Description of Shroud Test Samples

The DSS-13 shroud material is made from type ASTM 36 structural steel. As tabulated in [12], the chemical composition of this material, other than iron (Fe), is 0.26 percent maximum carbon, 0.04 percent maximum phosphorus, and 0.05 percent maximum sulfur. A 24- by 24-in. section of steel shroud material was obtained for purposes of cutting it into smaller test samples for cavity measurements. This 24- by 24-in. section was a discarded piece that had previously been cut out of a bypass-mode rectangular shroud to permit clearance of a 29-dB horn installed at the bypass focal point. This cutout panel section was made from the same material as the BWG center-pass shroud and is 0.2 in. thick. After several 4- by 4-in. square test samples were cut from the 24- by 24-in. piece, slight deviations from flatness were found to exist on the test samples, and therefore the two possible test surfaces were labeled convex and concave. When a test sample was placed on the cavity opening (diameter = 2.24 in.) the maximum deviation from a flat plane was less than 0.004 in. For the particular measurement technique employed, it is not critical that the test samples be perfectly flat. Small deviations from perfect flatness affect primarily the resonant frequency. However, care was taken to identify which side of the test samples were actually measured.

IV. Test Results

The test results are shown in Table 3 and are tabulated according to types of materials. The results of most interest to the BWG project are those for (1) the BWG shroud samples' painted and unpainted sides, (2) 6061 T6 aluminum with and without the zinc-chromate primer, (3) 6061 T6 aluminum with and without the primer and Triangle no. 6 paint, and (4) galvanized steel samples.

An average effective conductivity value of 0.01 mhos/m for the unpainted BWG shroud samples agrees favorably with other steel conductivity values shown in Table 1. Of particular interest is the effect of paint on the steel surfaces of the BWG shroud. Triangle Co. thermal diffusive paint no. 6 made the effective conductivity significantly worse. The effective conductivity changed from the unpainted test-sample value of 0.01×10^7 mhos/m to an average painted surface value of 0.0036×10^7 mhos/m. From this result, one might conclude that if the shroud's steel surfaces were covered instead with high-conductivity paint, the resulting conductivity would be significantly improved. However, when one of the shroud samples had the paint removed and then was repainted with silver paint, as may be seen in Table 3, the effective conductivity value of the silver-painted sample was only a factor of two times better than that of the unpainted sample.

Primer and paint on aluminum 6061 T6 surfaces made the conductivity values only slightly worse than those of

[2] Calculated from carbon steel curve plotted among other dc magnetization curves for various magnetic materials published by the General Engineering Laboratory of the General Electric Company.

the unpainted aluminum surfaces. Data on the loss of primer and paint are difficult to obtain. The paint loss data, obtained from cavity measurements and presented in this article, are probably much more accurate than the data obtained from radiometric measurements [13]. Another interesting result to note in Table 3 is the measured conductivities of the galvanized steel samples. The two galvanized steel samples tested had conductivity values close to those measured for a brass test sample. This surprising result indicates that galvanized steel should be seriously considered as a candidate shroud material.

Also shown in Table 3 are the corresponding noise temperatures that would be generated if a plane wave were normally incident on an infinitely large flat sheet of the sample material. The noise temperatures were calculated from the approximate formula

$$NT \cong \frac{4R_s T_p}{\eta_o} \tag{6}$$

where

η_o = free space impedance (120 π ohms)

T_p = physical temperature of the sheet (290 K)

It should be pointed out that these noise temperatures are not the same as the noise temperatures that would be generated due to conductivity losses when the material is used as the walls for a circular waveguide, such as a shroud.

V. Conclusions

Test data on the effective electrical conductivity of the DSS-13 shroud material have been presented. The painted shroud samples had an average effective conductivity of 0.0036×10^7 mhos/m. This conductivity value is about 140 times worse than the dc value of 0.5×10^7 mhos/m. The results of this study should prove useful in current investigations to determine the noise temperatures due to shroud dissipative losses. Other test data on various other types of steels and reflector surface materials have also been presented and should prove to be valuable for future reference purposes.

Acknowledgment

The authors thank Pablo Narvaez, of the JPL Reliability Engineering Section, for assistance in finding published information on the permeabilities of various types of steel.

References

[1] A. B. Vane, "Measurement of Effective Conductivity of Metallic Surfaces at 3000 Megacyles and Correlation with Surface Conditions and DC Conductivity," Stanford Microwave Laboratory Report No. 4, Palo Alto, California, pp. III–9, 1949.

[2] H. P. Westman, *ITT Reference Data for Radio Engineers (Fifth Edition)*, New York: Howard W. Sams, Inc., pp. 4–32, 1969.

[3] T. Y. Otoshi, C. T. Stelzried, B. C. Yates, and R. W. Beatty, "Comparisons of Waveguide Losses Calibrated by the DC Potentiometer, AC Ratio Transformer, and Reflectometer Techniques," *IEEE Trans. on Microwave Theory and Techniques*, vol. MTT-18, no. 7, pp. 406–409, July 1970.

[4] H. F. Reilly, J. J. Bautista, and D. A. Bathker, "Microwave Surface Resistivity of Several Materials at Ambient Temperature," *TDA Progress Report 42-80*, vol. October–December 1984, Jet Propulsion Laboratory, Pasadena, California, pp. 8–11, February 15, 1984.

[5] T. Otoshi, "H-band Cryogenic Load Development Plating Evaluation," *JPL Space Program Summary 37-28*, vol. 4, Jet Propulsion Laboratory, Pasadena, California, p. 153, August 31, 1964.

[6] R. C. Clauss and P. D. Potter, *Improved RF Calibration Techniques—A Practical Technique for Accurate Determination of Microwave Surface Resistivity*, Technical Report 32-1526, vol. 12, Table 1, Jet Propulsion Laboratory, Pasadena, California, p. 63, December 15, 1972.

[7] A. C. Beck, "Conductivity Measurements at Microwave Frequencies," *Proceedings of the IRE*, vol. 38, no. 10, pp. 1181–1189, October 1950.

[8] S. Ramo and J. R. Whinnery, *Fields and Waves in Modern Radio*, New York: John Wiley & Sons, 1950.

[9] R. D. Lending, "New Criteria for Microwave Component Surfaces," *National Electronics Conference Proceedings*, vol. 11, pp. 391–401, 1955.

[10] M. R. Gross, "Magnetic Permeability of So-Called Non-Magnetic Metallic Materials," *Journal American Science Naval Engineers*, vol. 66, no. 1, pp. 214–245, February 1954.

[11] E. H. Thom and T. Otoshi, "Surface Resistivity Measurements of Candidate Subreflector Surfaces," *TDA Progress Report 42-65*, vol. July and August 1981, Jet Propulsion Laboratory, Pasadena, California, pp. 142–150, October 15, 1981.

[12] American Society for Testing and Materials, *Annual Book of ASTM Standards*, "Standard Specification for Structural Steel," Designation A36/A 36M-90, vol. 01.05, Philadelphia, Pennsylvania, November 1990.

[13] T. Y. Otoshi and M. M. Franco, "Radiometric Tests on Wet and Dry Antenna Reflector Surface Panels," *TDA Progress Report 42-100*, vol. October–December 1989, Jet Propulsion Laboratory, Pasadena, California, pp. 111–130, February 15, 1990.

Table 1. Previously known or measured conductivity values of various types steel at dc and microwave frequencies.

Test sample	Surface roughness	Measurement method [Ref.]	Test freq., GHz	Effective conductivity, mhos/m	Square root of (dc cond./ eff. cond.)
Steel, cold rolled	Machined	[1, Tables]	dc	0.50×10^7	
Steel (0.4–0.5% C, balance Fe)	Unknown	[2, Table 12, pp. 4–22]	dc	0.769×10^7– 0.454×10^7	
Steel, cold rolled	Machined	Cavity [1]	3.015	0.0036×10^7	11.79
Stainless steel 430-2B	Rolled	Cavity [1]	3.015	0.0039×10^7	11.32
Type 303 stainless steel, test section 214	Electro-discharge machine (EDM) polished 8 μin.	JPL insertion loss (IL) and National Bureau of Standards (NBS) Reflectometer [3]	2.115 2.295 2.388 2.3985	0.019×10^7	5.13
Type 303 stainless steel test section 215	EDM polished 20 μin.	JPL insertion loss and NBS Reflect. [3]	2.295 2.388 2.3985	0.0136×10^7	6.06
Stainless steel, type 304	Polished <20 μin.	Cavity JPL [4]	8.400	0.1233×10^7	2.01
Stainless steel type 347	Polished <20 μin.	Cavity JPL [4]	8.400	0.0698×10^7	2.68
Mild steel	Polished <20 μin.	Cavity JPL [4]	8.400	0.0301×10^7	4.08
Stainless steel type 321	Polished <20 μin.	Cavity JPL [4]	8.400	0.0275×10^7	4.26
Stainless steel (type unknown)	Polished <20 μin.	Cavity JPL [4]	8.400	0.0075×10^7	8.16
Type 304 WR112 stainless steel section part no. UP-1	Seamless cold drawn tubing, 70–100 μin.	IL JPL [5]	8.448	0.0695×10^7	2.68
Type 304 WR112 stainless steel section UP-2	Same as UP-1 except inside electropolished, 20–35 μin.	IL JPL [5]	8.448	0.1187×10^7	2.05
Type 304 WR112 stainless steel section UP-3	Same as UP-1 except inside finished by a perfecto-peening process 35–45 μin.	IL JPL [5]	8.448	0.1066×10^7	2.17
Stainless steel (type unknown)	Unknown	Cavity JPL [6]	8.415	0.00757×10^7	8.13
Iron wire	Unknown	Cavity Bell Laboratories [7]	9.000	0.148×10^7	1.84

Table 2. Chemical compositions and relative permeabilities of various types of stainless steels at 24 deg C (selected data from Tables IX and X of [10]).

AISI[a] type stainless steel	Chemical composition, percent										Relative permeability for magnetizing forces of	
	C	S	P	Mn	Cr	Ni	Mo	Cu	Al	Other	H = 0.5 Oe	H = 100 Oe
303 annealed, machined	0.05	0.259	0.031	0.67	0.49	18.42	8.55	—	—	—	1.10	1.03
304 bar	0.073	0.030	0.037	1.03	0.47	18.87	8.47	0.30	0.24	—	<1.02	1.00
321 for plate thicknesses:												
5/8–1.0 in.	0.05	0.012	0.037	1.55	17.96	9.67	0.24	0.31	—	Ti 0.41	—	1.46–1.70
5/8 in.	0.05	0.006	0.032	1.22	17.35	9.83	0.22	0.18	—	Ti 0.39	—	1.06
5/8 in.	0.06	0.010	0.040	1.40	17.60	9.85	0.17	0.32	—	Ti 0.41	—	1.01–1.02
347 wrought pipe	0.08	0.010	0.020	1.69	18.13	12.34	—	—	—	Cb 0.80	<1.02	1.00

[a] American Iron and Steel Institute.

Table 3. Test results of X-band cavity measurements.[a]

Sample run ID	Run no.	Description	Side tested	Surface roughness, μin.	f_o, GHz	R_s, ohms/square	Effective cond., mhos/m	Flat sheet noise temp, K[b]
Silver	1–6	Cavity ref. plate			8.421883	0.0270[c]	4.557×10^7	0.083
UP1CLR		BWG antenna shroud ASTM A36 steel sample no. 1, paint removed	Convex	230	8.420669	0.5993	0.0093×10^7	1.844
UP2CLR	1	BWG antenna shroud ASTM A36 steel sample no. 2, paint removed	Convex	>250	8.410031	0.5479	0.0111×10^7	1.686
UP2CLR	2	Same as above repeat test	Convex	>250	8.421861	0.5806	0.0099×10^7	1.787
UP3CLR		BWG antenna shroud ASTM A36 steel sample no. 3, paint removed	Concave	200	8.404988	0.5723	0.0101×10^7	1.761
UP4CLR		BWG antenna shroud ASTM A36 steel sample no. 4, paint removed	Concave	210	8.405010	0.5926	0.0095×10^7	1.823
UP1PNT		BWG antenna shroud ASTM A36 steel sample no. 1, plus Triangle 6 paint	Concave	134	8.406965	1.1184	0.0027×10^7	3.441
UP2PNT		BWG antenna shroud ASTM A36 steel sample no. 2, plus Triangle 6 paint	Concave	93	8.402868	0.9917	0.0034×10^7	3.051
UP4PNT		BWG antenna shroud ASTM A36 steel sample no. 4, plus Triangle 6 paint	Convex	156	8.403963	0.8353	0.0048×10^7	2.570
UP4SVR	1	BWG antenna shroud ASTM A36 steel sample no. 4, Triangle 6 paint removed and steel surface is now silver painted	Concave		8.407994	0.4913	0.0138×10^7	1.512
UP4SVR	2	Same as (UP4SVR, Run 1) above except silver paint allowed to dry longer	Concave		8.410720	0.3891	0.0219×10^7	1.197

[a] Measurements were made on August 9, 1991.

[b] This is the noise temperature when the material is used as a flat plate short for normal incidence [see Eq. (6)]. This value is not the same as the noise temperature generated when this material is used as a BWG shroud.

[c] Average of six runs.

Table 3 (cont'd)

Sample run ID	Run no.	Description	Side tested	Surface roughness, μin.	f_o, GHz	R_s, ohms/square	Effective cond., mhos/m	Flat sheet noise temp, K[b]
COLDROLL		0.047-in.-thick cold rolled steel sheet	Side 1 Side 2	44 67	8.423088	0.3708	0.0242×10^7	1.141
COPPER	1	0.064-in. thick copper sheet	Side 1 Side 2	30 26	8.421679	0.0281	4.202×10^7	0.086
COPPER	2	Same as above except repeat test	Side 1 Side 2	30 26	8.420993	0.0275	4.388×10^7	0.085
COPPER	3	Same as above except repeat test	Side 1 Side 2	30 26	8.421060	0.0293	3.871×10^7	0.090
TYO1CLR	1	0.070-in. thick 6061-T6 Al sheet from DSS 13, bare metal side	Side 1	23	8.413483	0.0353	2.670×10^7	0.109
TYO1CLR	2	Same as TY01CLR above except repeat test	Side 1	23	8.426800	0.0386	2.234×10^7	0.119
TYO1PMR	1	0.070-in. thick 6061-T6 Al sheet plus primer (primer is zinc-chromate side, ~ 0.6 mil)	Side 2 (other side of TYO1CLR)	64	8.409008	0.0378	2.321×10^7	0.116
TYO1PMR	2	Same as TYO1PMR above except repeat test	Side 2 (other side of TYO1CLR)	64	8.423660	0.0409	1.992×10^7	0.126
TYO2CLR	1	0.070-in. thick 6061-T6 Al sheet from GTS, bare metal side	Side 1	32	8.416702	0.0371	2.412×10^7	0.114
TYO2CLR	2	Same as above except repeat test	Side 1	32	8.426176	0.0381	2.289×10^7	0.117
TYO2PNT		0.070-in. thick 6061-T6 Al sheet primer plus Triangle no. 6 paint (measured thickness of primer plus paint ~ 1.1 mil)	Side 2 (other side of TYO2CLR)	89	8.420514	0.0439	1.722×10^7	0.135
TYO4CLR		0.063-in. thick 6061-T6 Al sheet bare metal side	Side 1	16	8.427346	0.0388	2.210×10^7	0.119
TYO4PNT		0.063-in. thick 6061-T6 Al sheet plus primer plus old Triangle no. 6 paint (measured thickness of primer plus paint ~ 1 mil)	Side 2 (other side of TYO4CLR)	26	8.425368	0.0399	2.086×10^7	0.123

Table 3 (cont'd)

Sample run ID	Run no.	Description	Side tested	Surface roughness, μin.	f_o, GHz	R_s, ohms/square	Effective cond., mhos/m	Flat sheet noise temp, K[b]
ALUM		0.064-in. thick 6061 Al sheet	Side 1 Side 2	10 10	8.424538	0.0390	2.182×10^7	0.120
BRASS		0.063-in. thick brass sheet	Side 1 Side 2	14 21	8.424703	0.0492	1.372×10^7	0.151
DB3S		0.024-in. thick galvanized steel sample	Side 1 Side 2	22 23	8.426146	0.0526	1.201×10^7	0.162
TYO3		0.048-in. thick, galvanized steel sample from DSS 13	Side 1 Side 2	25 23	8.425480	0.0476	1.466×10^7	0.146

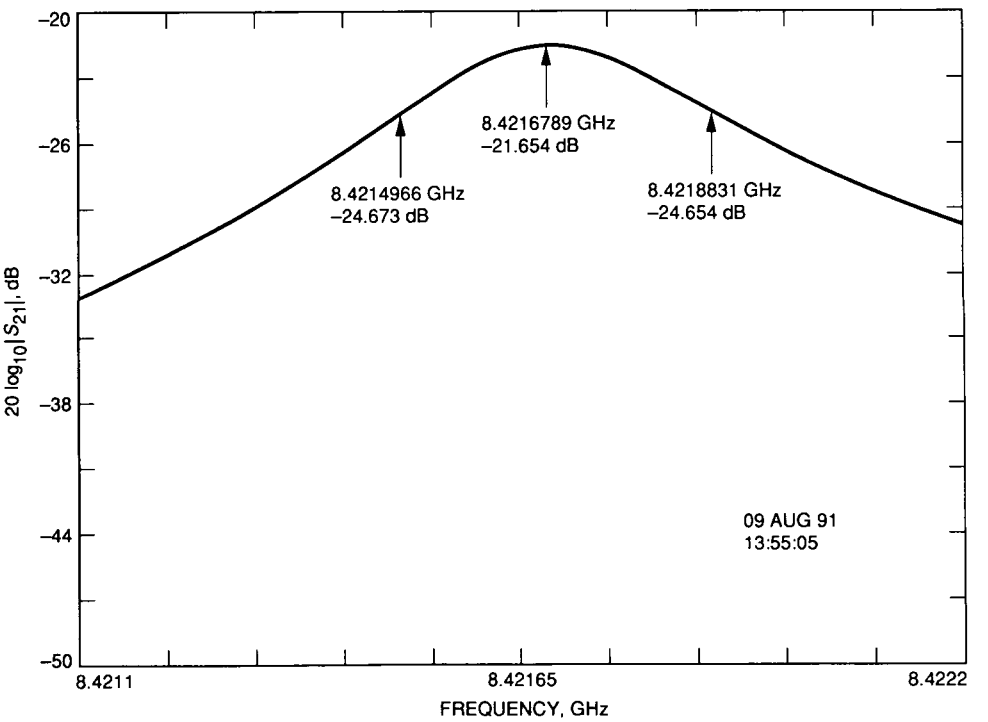

Fig. 1. Example of an automatic network analyzer plot of cavity-method insertion measurements on a copper test sample.